presented for comparison. The agreement is good, although the comparison strictly speaking is not appropriate, since the experimental data were obtained at $M_\infty = 3$ to 5, $p_\infty = 1$ atm. Least-squares fit relations are presented for the 3-in. sphere data on Fig. 2 together with those of Murphy and Dickinson for their $\frac{1}{8}$- and $\frac{1}{4}$-in.-diam sphere data. The agreement is reasonable so that there does not appear to be any pronounced size effect, even though the projectile size factor is up to 12.

From the results it can be concluded that, if the wake width data for the 3-in.-diam spheres are averaged over stretches of approximately 5 body diameters in length, the growth rate can be represented by an $(x/d)^{1/2}$ relationship for the entire length of the wake.[5] However, an $(x/d)^{1/3}$ growth relationship can also be used, and it would seem more appropriate to use such a relationship, since the theoretical analyses of the turbulent wake predict this form of growth, whereas none predict the $(x/d)^{1/2}$ relationship. In particular, the analysis of Lees and Hromas for the turbulent wake predicts a growth rate that is in good agreement with the data of this investigation when such data are viewed in the light of an $(x/d)^{1/3}$ growth form. The agreement is good even to the extent of showing the region of the inflection point in the growth curve beyond which there is an increase in the growth rate. This phenomenon arises as a result of the marked increase in the turbulent viscosity when the turbulent front has reached the cooler, denser gas with the high enthalpy gradients in the inviscid flow.

Although the 3-in.-diam spheres represent a factor of up to 12 from the sphere firings at other laboratories, no obvious scaling effect is apparent in the growth rate of the turbulent inner wake, at this pressure and in this Mach number region, when the results are compared.

References

[1] Slattery, R. E. and Clay, W. G., "Width of the turbulent trail behind a hypervelocity sphere," Phys. Fluids **4**, 1199–1201 (October 1961).

[2] Dana, T. A. and Short, W. W., "Experimental study of hypersonic turbulent wakes," Convair Rept. ZPh-103A (August 1961).

[3] Lees, L. and Hromas, L., "Turbulent diffusion in the wake of a blunt-nosed body at hypersonic speeds," J. Aerospace Sci. **29**, 976–993 (August 1962); also Space Technology Labs., Aerodynamics Dept., R-50 (July 1961).

[4] Murphy, C. H. and Dickinson, E. R., "Growth of the turbulent wake behind a supersonic sphere," AIAA J. **1**, 339–342 (1963).

[5] Knystautas, R., "The growth of the turbulent inner wake behind a 3 inch diameter sphere," Canadian Armament Research and Development Establishment TR 488/64 (February 1964).

Effect of Shock Curvature on Turbulent Heating of Sphere-Cones

C. T. EDQUIST*

Lockheed Missiles and Space Company, Sunnyvale, Calif.

Nomenclature

a = speed of sound, fps
C_D = Newtonian nose drag coefficient
C_m = compressibility function [Eq. (7)]
M = Mach number
Pr = Prandtl number
q = convective heat-transfer rate
R_n = nose radius, ft
r = dimensionless body radius
s = dimensionless surface location
t = dimensionless distance from body surface
u = velocity, fps
x = dimensionless axial location
y = dimensionless shock coordinate
z = altitude, ft
δ = dimensionless boundary-layer thickness
θ_c = cone half-angle, deg
θ_{cs} = conical shock angle, deg
μ = viscosity, lbm/ft-sec
ρ = density, lbm/ft^3
ϕ_T = function defined by Eq. (6)
ψ = stream function defined by Eq. (2)

Subscripts

c = cone
e = boundary-layer edge condition
ns = emanating from a normal shock
∞ = freestream condition
$*$ = reference condition

Received April 13, 1964.

* Senior Thermodynamics Engineer. Member AIAA.

A RECENT note[1] presented a simple method for estimating shock curvature effects on the outer edge conditions of a laminar boundary layer. The method was applied to a sphere-cone configuration with the results indicating a significant increase in convective heating over levels computed on the basis of flow emanating through a normal shock. Since, for most re-entering bodies, the majority of the heat pulse occurs with a turbulent boundary layer, an easily applied procedure for determining shock curvature effects in this case is perhaps even more important.

Following the general approach of Ref. 1, a method is developed for determining the shock curvature effects on a zero pressure gradient turbulent boundary layer. Only axisymmetric flows are considered, and the laminar portion of the boundary layer preceding the turbulent is neglected. Then, from continuity considerations,

$$\rho_\infty u_\infty y^2 = 2[\psi(s, \delta)/R_n{}^2] \tag{1}$$

with

$$\frac{\psi(s, \delta)}{R_n{}^2} = \int_0^\delta \rho u r dt \tag{2}$$

where all lengths are normalized with respect to the nose radius R_n. Following established methods[2] and assuming a $\frac{1}{7}$ power law variation of ρu through the boundary layer, i.e.,

$$\rho u/\rho_e u_e = (t/\delta)^{1/7} \tag{3}$$

then

$$\psi(s, \delta)/R_n{}^2 = \tfrac{7}{8}\rho_e u_e r \delta \tag{4}$$

where the boundary-layer thickness can be represented by

$$\delta = \frac{0.382}{Pr^{2/3}} \frac{R_n{}^{-1/5}}{\rho_* u_e r} \left[\int_0^s \rho_* u_e \mu_*{}^{1/4} r^{5/4} ds\right]^{4/5} \tag{5}$$

Combining Eqs. (1, 4, and 5) yields the relation

$$r^{5/4}\frac{ds}{dy} = \phi_T(y, \rho_*/\rho_e) = 3.12 R_n{}^{1/4}\left(\frac{\rho_\infty a_\infty}{\mu_\infty}\right)^{1/4} \times M_\infty{}^{5/4} C_m \frac{y^{3/2}}{(\rho_e/\rho_\infty)(u_e/a_\infty)(\mu_e/\mu_\infty)^{1/4}}\left[1 + \frac{1}{2}\frac{d\ln\rho_*/\rho_e}{d\ln y}\right] \tag{6}$$

with

$$C_m = [(\rho_*/\rho_e)(\mu_e/\mu_*)]^{1/4} \tag{7}$$

Equation (6) (in direct correspondence with the laminar relation given in Ref. 1) connects the shock-wave coordinate y with the body coordinate s through the boundary-layer edge conditions. A direct solution of the problem is available if three conditions can be met: first, the body surface pressure is constant; second, the quantity C_m is constant; and, finally, the second term in the brackets in Eq. (6) is zero indicating ϕ_T is a function of y only. For sphere-cones, the pressure gradient is nearly zero over the range in which the shock

curvature effects predominate. Aposteriori evaluation of the other two assumptions will provide an estimation of their importance.

In addition, the shock shape must be known. For sphere-cones, the shock correlation of Ref. 3 is

$$\frac{y}{\cos\theta_c} = 1.424\left[C_D^{1/2}\frac{x}{\cos\theta_c}\right]^{0.46} \tag{8}$$

which is faired into the conical shock angle given by the correlation

$$\sin\theta_{cs} = 1.01\sin\theta_c + (0.536/M_\infty) \tag{9}$$

The tangent point is

$$\frac{y}{\cos\theta_c} = \left[\frac{0.984C_D}{\tan^2\theta_{cs}}\right]^{0.426} \tag{10}$$

To apply the method, the properties immediately behind the shock are determined for several values of y up to the straight portion of the shock. Expanding these conditions isentropically to the assumed constant sphere-cone pressure, the boundary-layer edge parameters are determined for some unknown s. The shock wave and isentropic expansion calculations can be done for either perfect or real gases; however, the calculations of this note are confined to the perfect gas case. These values are used to calculate $\phi_T(y)$ from Eq. (6). Then,

$$\int_0^s r^{5/4}ds = \int_0^y \phi_T(y)dy \tag{11}$$

Since, for sphere cones,

$$r = \cos\theta_c + \left(s - \frac{90 - \theta_c}{180}\pi\right)\sin\theta_c \tag{12}$$

the left side of Eq. (11) can be integrated directly to yield finally

$$r^{9/4} = \left(\cos\theta_c - \frac{90 - \theta_c}{180}\pi\sin\theta_c\right)^{9/4} + \frac{9\sin\theta_c}{4}\int_0^y \phi_T(y)dy \tag{13}$$

which is easily solved for r and thus s.

The preceding equations were applied to a 15° half-angle sphere-cone with a 3-in. nose radius at an altitude of 50,000 ft and a Mach number of 20. C_m was taken equal to 1. Figure 1 shows the variation of boundary-layer edge Mach number along the body for a perfect gas. The conical value is attained at an actual surface location of about 79 in. Examination of Eq. (6) shows that the nose radius effect is simply a multiplicative constant. Thus, if the nose radius is halved, the conical Mach number is reached at an actual surface location of 36 in., a considerable effect. For perfect gas calculations, the altitude effect is also confined to the constant, and changing the altitude to 100 kft reduces the conical Mach number location to 59 in., a smaller but still significant change. Thus, as expected, decreasing the nose radius and increasing the altitude compound the shock curvature problem.

The effects of the assumption of constant C_m and the variation of ρ^*/ρ_e over the body were evaluated aposteriori. The

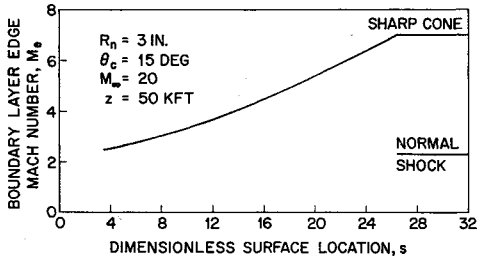

Fig. 1 The distribution of boundary-layer edge Mach number along a sphere-cone.

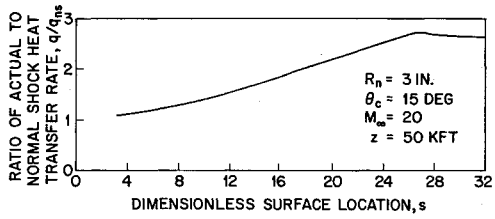

Fig. 2 The distribution of cold wall turbulent heat-transfer rate along a sphere-cone.

cold wall value of C_m varied less than 25% from the conical value to that for boundary-layer edge emanation from a normal shock. The average value was slightly greater than 1. This variation increased the surface location at which cone flow began by less than 3%. Evaluating the second term in the brackets of Eq. (6) caused a decrease of less than 10% in the surface location at which cone flow was established. The two effects are of opposite sign for the present case, thus minimizing their importance. Although the effect of the present assumptions are not insignificant, it is felt that meaningful results can still be obtained.

The cold wall heat-transfer rate, normalized to that expected for boundary-layer edge emanation from a normal shock, is presented in Fig. 2. Although increases of 30 to 40% in heat-transfer rate are expected for a similar laminar case,[1] the turbulent results indicate factors of from 2 to 3. This effect should be easily discernible (unlike the smaller laminar effect) in experimental data. Unfortunately, few turbulent data exist for sphere-cones. The magnitude of the values herein emphasize the need for such data.

References

[1] Rubin, I., "Shock curvature effects on the outer edge conditions of a laminar boundary layer," AIAA J. 1, 2850–2852 (1963).

[2] Bromberg, R., Fox, J. L., and Ackermann, W. G., "A method of predicting convective heat input to the entry body of a ballistic missile," Ramo-Woolridge Corp., Los Angeles, Calif. (June 1956); confidential.

[3] Klaimon, J. H., "Bow shock correlation for slightly blunted cones," AIAA J. 1, 490–491 (1963).

Improved Calculation of Vacuum Vertical Trajectories

Leo B. Schlegel* and Philip J. Bonomo*
International Business Machines Corporation, Bethesda, Md.

Introduction

In preliminary trajectory analysis, vacuum vertical trajectories are often employed as approximations or limiting cases. Examples are idealized sounding rocket trajectories, lunar landing descent paths, limiting minimum time transfers between coplanar circular orbits, etc. When the over-all altitude variation for such a trajectory is small, the approximation of constant gravitational acceleration is usually made to facilitate calculation of velocity and altitude time histories. At modest additional effort, however, these calculations can be based on an inverse-square gravity field and hence made more nearly exact. The appropriate formulation is a limiting version of Lambert's theorem for transfer time between two radii on a Keplerian ellipse, a vacuum vertical trajectory being

Received April 13, 1964; revision received May 8, 1964.

* Advisory Engineer, Federal Systems Division. Member AIAA.